

Electrical Characterization of Isotropic Conductive Adhesive under Mechanical Loading

ZHIMIN MO,^{1,2} XITAO WANG,¹ TIEBING WANG,¹ SHIMING LI,¹
ZONGHE LAI,¹ and JOHAN LIU¹

1.—Division of Electronics Production, School of Mechanical and Vehicular Engineering, Chalmers University of Technology, S-412 96 Gothenburg, Sweden. 2.—E-mail: zhimin.mo@me.chalmers.se

Isotropic conductive adhesive (ICA) is a strong candidate for replacing toxic lead-based solders. Before wide application of this new technology can occur, the degradation mechanisms must be thoroughly understood. In this work, we investigated the electrical characteristics of a commercial ICA under mechanical loading. The results showed that the resistance rose monotonically with the joint strain in the lap shear test, while it increased steadily with the number of cycles in the low-cycle fatigue test. To elucidate the experimental observations, two-dimensional finite-element modeling (FEM) was carried out, and the effects of mechanical loading on the initial intimate interaction among silver fillers were analyzed. Additionally, based on modeling, the possible electrical degradation mechanisms were discussed.

Key words: Electrical conductive adhesive, low-cycle fatigue, degradation mechanism

INTRODUCTION

Isotropic conductive adhesives (ICAs) have been applied to electronics packaging for decades. New products are being continuously introduced to replace toxic lead-based solders. Even compared with lead-free solders, ICA has some advantages, for instance, lower curing temperature and the possibility of bonding nonsolderable substrates.¹

The ICA pastes are generally formulated by mixing epoxy resin with metallic fillers. The most popular fillers are silver flakes because of their good electrical performance, stability, and the inherent conductivity of silver oxides. Instead of the metallurgical connection, the electrical conduction of the ICA joint is based on the mechanical contacts among silver flakes that form a network (conductive chain) to transfer electrons. Both matrix-filler and filler-filler interactions govern the performance of the joint, and any factors affecting the initial intimate interaction among silver flakes will surely influence its reliability.

Similar to a solder joint, ICA joints must be able to withstand thermal stress resulting from the thermal expansion mismatch between the substrate and chip during the lifetime. Due to the temperature

fluctuation caused by the device power on/off cycles, thermomechanical fatigue is considered to be one of the primary failure mechanisms. Therefore, thermal cycling tests are used widely to evaluate the reliability of ICA joints.^{2,3} Unfortunately, this kind of test is very time consuming and the final results are affected by many factors. Some cyclic mechanical tests^{4,5} were developed to rapidly test and assess the creep failure life. Furthermore, in mechanical tests, the joint can be strained in a controlled manner, which is very helpful for failure analysis. Constable et al.⁵ tested the low-cycle fatigue properties of four types of commercial ICAs and found that their electrical resistances increased with the number of cycles, which was mainly attributed to the loss of interface electrical contacts.

The present study focuses on the electrical performance of a commercial ICA joint under mechanical loading. To gain insight into the electrical degradation mechanism, finite-element modeling (FEM) was executed, and the effects of mechanical loading on the initial intimate interaction among silver fillers were analyzed.

EXPERIMENTAL PROCEDURE AND RESULTS

The ICA paste for this study was supplied by Micro Joining AB (Tyresö, Sweden). One cured joint was

(Received February 26, 2002; accepted June 21, 2002)

cross-sectioned and the morphology was observed with a scanning electron microscope (SEM). As can be seen from Fig. 1, the joint contains a mixture of silver flakes with varied sizes.

All samples for mechanical tests were single joint lap shear specimens comprised of two FR4 boards bonded with an ICA joint (Fig. 2). The ICA paste was deposited using a hand dispenser on the gold-metalized copper pad of one FR4 board, and a second board with the same pad was aligned to the first with a jig. The thickness of the joint was controlled to 0.4 mm by spacers. Once the FR4 boards were bonded in the jig, the joint was cured in an oven at 150°C for 30 min and then cooled to room temperature outside the oven.

Both a lap shear tensile test and a low-cycle fatigue test were performed using a load frame. A data acquisition/switch unit was used to monitor the changes of the joint resistance during mechanical tests, and the four-probe technique was chosen for these measurements.

To assess the effects of shear deformation on elec-

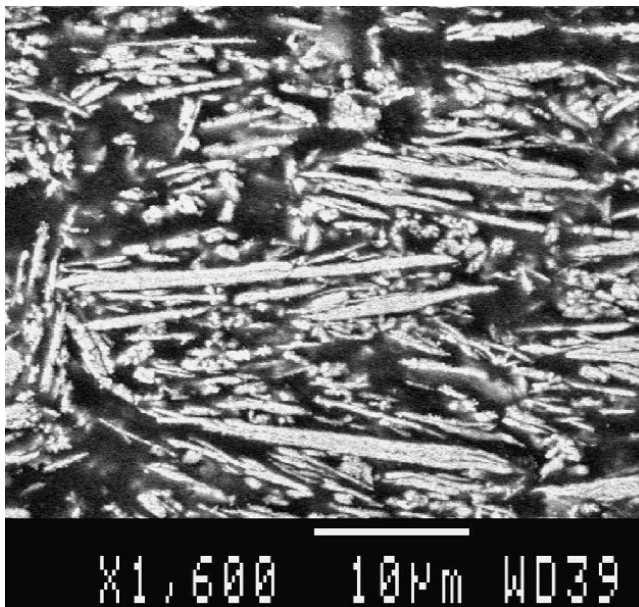


Fig. 1. SEM micrograph of an ICA joint's cross section. Silver fillers show white contrast.

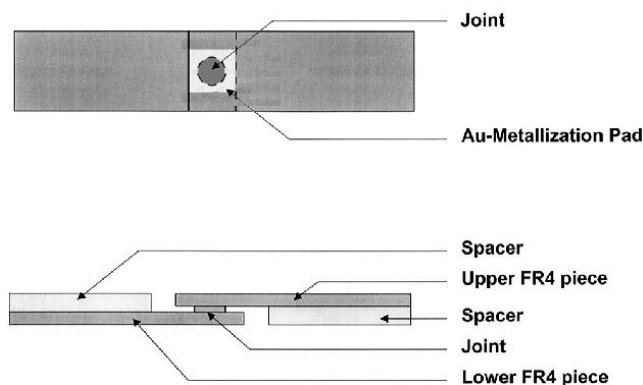


Fig. 2. Configuration of samples used for mechanical tests.

trical performance, samples were subjected to a lap shear tensile test. The strain was limited to the elastic regime and the joint resistance was scanned at both loading and unloading stages. The speed of the crosshead was kept at 0.002 mm/min to obtain sufficient data. Figure 3 shows the typical resistance change of the ICA joint with test time. Each point represents the statistic average of data collected in a period of 2 min. For comparison, the variation of external load applied on the sample is also plotted at the lower part of the figure. It is worth noting that the crosshead displacement included the deformation of both ICA joint and FR4 boards. Compared with the gauge length of the sample, the size of the joint was quite small. The real strain in the joint was only a fraction of the total deformation.

By comparing two curves in the figure, one can easily see that the resistance of the joint increased monotonically with the external load. As the deformation occurred in the elastic regime, the strain was linear with stress. Therefore, the load could be used to represent the strain of the joint, and it can be concluded that the conductivity of the joint decreases as the applied shear strain increases. Also, the conductivity recovered almost completely once the load was removed. This indicates that the damage to the joint was very limited during one cycle of elastic shear strain.

The same specimen geometry was used for low-cycle fatigue tests conducted at room temperature. The crosshead displacement was the control variable and the frequency was 0.2 Hz. A triangular waveform was chosen because it gives a constant strain rate. For comparison with the result from the lap shear tensile test, samples were loaded to the same maximum displacement, and the minimum displacement was set as zero. The electrical resistance was measured once per cycle. Figure 4 shows the typical electrical resistance variation with the number of cycles. Similar to Ref. 5, the resistance was stable in the beginning, but then increased gradually with the

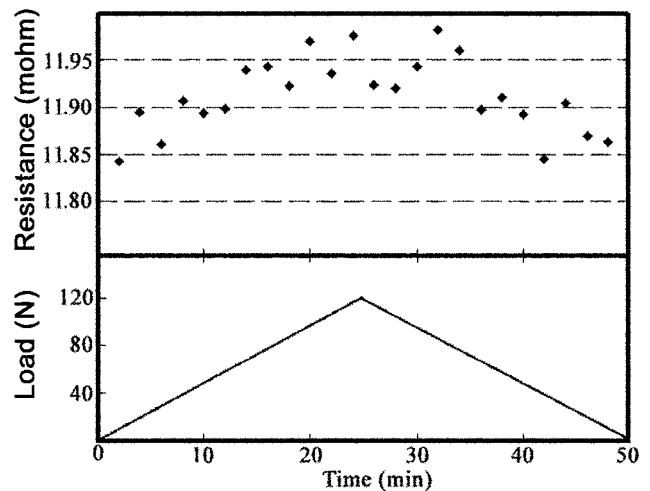


Fig. 3. Time dependency of joint resistance and external load in the lap shear test. The monotonic relationship between resistance and load is evident.

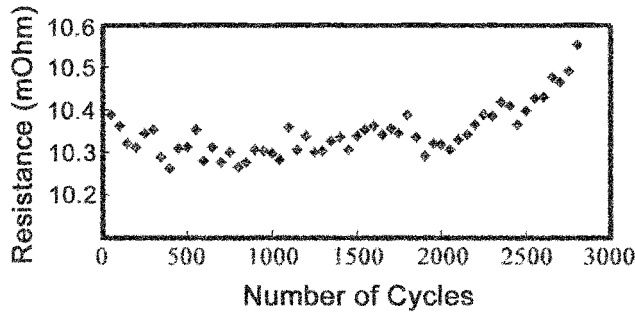


Fig. 4. Variation of joint resistance with number of cycles during the low-cycle fatigue test. Each data point represents the statistical average of 50 cycles.

number of cycles, indicating some degree of damage to the conductive joint accumulated during the test.

FEM AND DISCUSSION

The ICA joint consists of metallic fillers and epoxy matrix. In general, each metallic filler is surrounded by other fillers, as well as by an epoxy matrix. Due to the complex filler-filler and filler-matrix interactions, it is quite difficult to calculate the stress distribution without any simplification. The present modeling is based on the Mori-Tanaka's approach,⁶ assuming that the average stress/strain in the fillers can be approximated by that of embedding a single filler into an infinite matrix subjected to the average matrix stress/strain. To gain insight into the average filler-filler interaction, as well as the filler-matrix interaction, the ICA joint was simplified into a double-filler system, i.e., only a pair of fillers embedded in an infinite matrix was considered. Since the filler-pad interaction is similar to that between fillers, the present modeling may also shed some light on the degradation of anisotropic conductive adhesive under cyclic loading.

Figure 5 shows the configuration of the simplified model in which the large epoxy matrix surrounds two contacting rectangular silver fillers. The dimension of the conductive joint was set as $20\ \mu\text{m} \times 20\ \mu\text{m}$. The height of fillers was $1\ \mu\text{m}$, while the contact length (representing the contact area projected onto the strain direction) was $2\ \mu\text{m}$. The fillers were bonded perfectly to the matrix, but no bonding between fillers was assumed. Since the resin shrinkage is quite small⁷ and debonding occurs readily between close-spaced fillers,⁸ this simplification is not so far from the actual situation. As a further simplification, neither surface tarnish nor lubricant between the fillers was assumed in the present modeling.

An appropriate mesh was used, with a finer mesh in the region around fillers. A total of approximately 3600 elements were needed for this preliminary

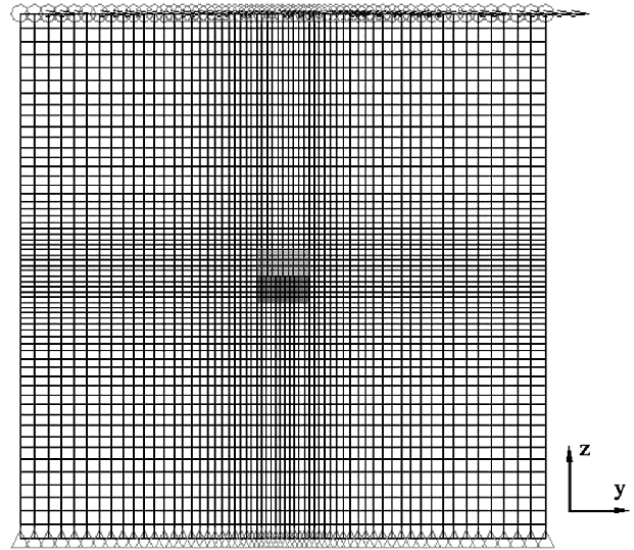


Fig. 5. Configuration of the simplified model for FEM calculations. Only two contacting silver fillers (gray) embedded in a large epoxy matrix (white) were considered.

study. The calculation was carried out with a two-dimensional plane strain condition. As the strain in the entire joint was quite small, we only considered the plasticity of the epoxy matrix, and the deformation of the silver filler was regarded as elastic. The mechanical properties of two employed materials are given in Table I.

The joint was hinged at the lower surface, while the upper surface could roll only along the y-axis. A displacement with $0.16\ \mu\text{m}$ along the y-axis, corresponding to 0.8% average shear strain, was imposed on the upper surface.

Figure 6 gives the von Mises stress distribution in and around the silver fillers. Due to the introduction of the separable contact surface, the otherwise uniform inclusion stress distribution has changed considerably. The stress in fillers is released near the contact region and almost equals zero in the middle of the contact surface. On the other hand, the matrix stress, as well as the inclusion stress, concentrates around the tips of the contact surface. Because silver possesses a higher yield strength than the epoxy matrix, plastic strain occurs readily in the matrix, which triggers the initiation of the microcracks. Theoretical calculations⁹ and experimental observation¹⁰ on particulate-reinforced composites pointed out that the broken reinforcements would act as the source of microcracks. The present calculation indicates that the separable mechanical contact between fillers may play a similar role in the degradation of the ICA joint. Furthermore, the propagation

Table I. Material Properties for FEM Calculations

| Material | Elastic Modulus | Poisson's Ratio | Yield Strength | Strain Hardening Modulus |
|----------|-----------------|-----------------|----------------|--------------------------|
| Epoxy | 3 GPa | 0.4 | 60 MPa | 200 MPa |
| Silver | 76 GPa | 0.37 | — | — |

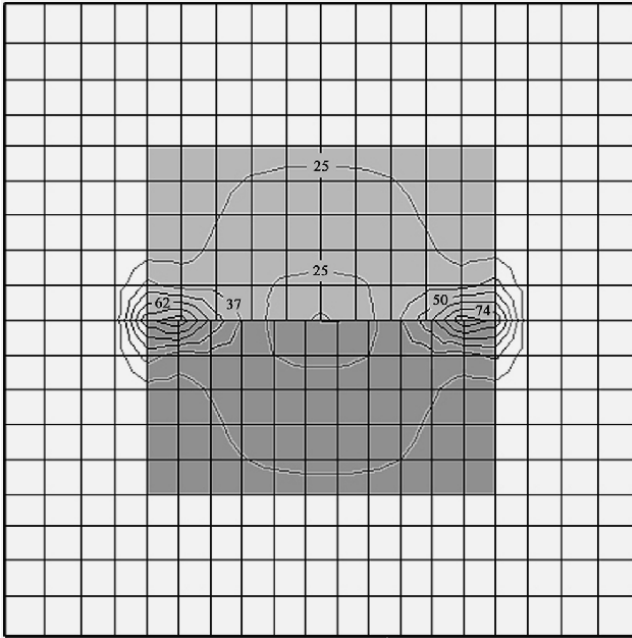


Fig. 6. Distribution of von Mises stress (MPa) in and around silver fillers.

of microcracks in the matrix weakens the constraint on the fillers, loses the initial intimate contact, and thus increases the electrical resistance.

In the present modeling, the contacting fillers separate and a gap forms (Fig. 7) when the joint is subjected to shear strain. Because our calculation ignored the interaction between fillers, this result should be regarded as a motion tendency of the fillers. Considering that the actual contact surface sustains compression resulting from resin shrinkage, the separation tendency decreases the compressive force between fillers. Since the electrical conduction of the ICA joint results from this contact pressure,^{11,12} the shear strain on the joint reduces its electrical conductivity. However, if there is not permanent damage to the adjacent matrix, the intimate contact between fillers will recover after the external load is removed, and so will the electrical resistance. This result agrees qualitatively with what is observed in the lap shear tensile test.

Interfacial sliding has been observed in composite

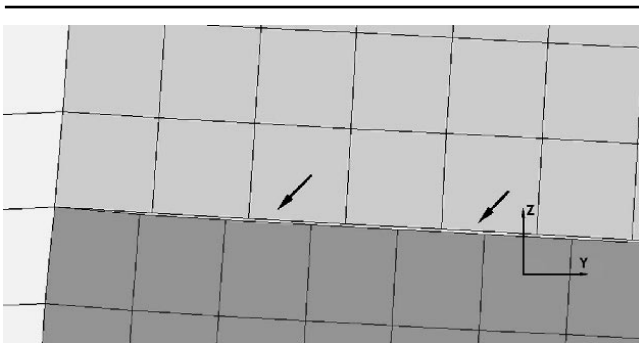


Fig. 7. Enlarged area around a tip of the contact region. A gap (pointed with arrows) forms between fillers when the joint is subjected to shear strain.

materials under cyclic loading.^{13,14} Present modeling also shows probable relative sliding between fillers. Figure 8 illustrates the linear relationship between the sliding displacement and the joint strain. Again, this calculated result only presents a tendency of the filler's movement. If the strain is large enough and the driving force on fillers exceeds the blocking (for instance, the mechanical interlock) on the contact surface, interfacial sliding will start. The stress concentration around the tips of the contact surface is closely related to the sliding. The larger the blocking force on the contact surface, the smaller the sliding displacement, and thus the smaller the stress concentration.

Interfacial sliding has a great influence on the reliability of the conductive joint under cyclic loading. Due to the sliding, old contact points will be worn out, while new points will be created. These two processes can keep a dynamic balance in the beginning of the cyclic test, so the resistance remains stable. Polishing of the contact surface will gradually reduce the real contact area, resulting in degradation of the electrical conductivity. On the other hand, the polishing decreases the blocking against sliding and thus increases the stress concentration around the tips of the contact surface between fillers. This also promotes the initiation of microcracks and worsens the electrical performance. The dominant mechanism for ICA joints under cyclic loading is still open to question.

Numerical calculations with different filler dimensions have also been performed. As ICA joints with silver flakes have better electrical performance than those with sliver particles, only rectangular fillers were considered. Besides that mentioned above, four other filler sizes were chosen: two with a contact length of 2 μm and the other two with a length of 4 μm . Fillers with the same contact length could be categorized with their aspect ratio (contact length/height of filler). Table II shows the effect of filler dimension on stress concentration and sliding displacement. As can be seen, neither concentrated stress nor relative displacement shows an obvious relationship with the aspect ratio. Instead, they depended strongly on the contact length between fillers.

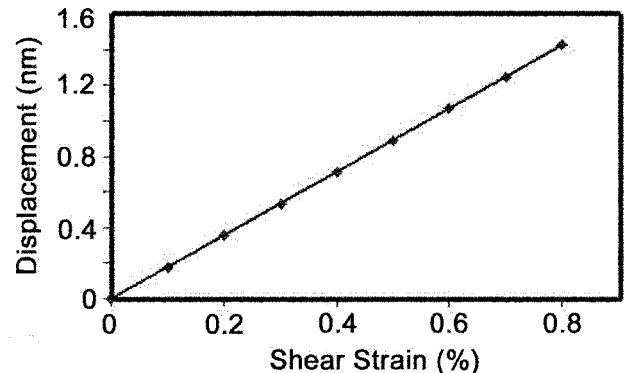


Fig. 8. Calculated sliding displacement between fillers as a linear function of shear strain of the joint.

Table II. Calculated Highest von Mises Stresses around Contact Surface Tips and Relative Sliding Displacements with Different Filler Dimensions

| | | | | | |
|----------------------------------|-----|-----|-----|-----|-----|
| Contact length (μm) | 2 | 2 | 2 | 4 | 4 |
| Height (μm) | 1 | 2 | 4 | 2 | 4 |
| Aspect ratio | 2 | 1 | 0.5 | 2 | 1 |
| Highest stress (MPa) | 98 | 95 | 85 | 188 | 188 |
| Displacement (nm) | 1.4 | 1.3 | 1.2 | 3.6 | 3.6 |

As the contact length doubled (from 2 μm to 4 μm), the highest stress increased about 2 times and the relative displacement increased more than 2.5 times.

CONCLUSIONS

The electrical resistance change of a commercial ICA joint was measured during both lap shear tensile test and low-cycle fatigue test. At either the loading or unloading stage of the tensile test, the resistance varied monotonically with the joint strain, and the conductivity recovered almost completely after the elastic load was removed. In the fatigue test, the resistance increased with the number of cycles.

To gain insight into the electrical degradation mechanism, a model with two contacting silver fillers embedded in epoxy matrix was then constructed and two-dimensional FEM calculations were carried out. The results revealed three important features elucidating the experimental observations.

- The stress concentrates around the tips of the contact surface between fillers, indicating the sites where microcracks would initiate readily. The propagation of microcracks weakens the constraint applied on the fillers and decreases their intimate contact.
- Fillers tend to separate when shear strain is applied to the adhesive joint, which decreases the contact pressure between fillers and thus increases the joint resistance. But, after the external load is removed, this separation will recover if no permanent damage occurs in the adjacent epoxy matrix.
- Fillers probably slide along the contact surface when the joint is under cyclic loading, which reduces the real mechanical contact area and pro-

motes the propagation of microcracks. Consequently, the joint resistance would rise steadily with the number of cycles.

In addition, numerical simulation also revealed that both stress concentration and relative motion of fillers depend strongly on the dimension of separable contact surface, while the influence of the filler's aspect ratio is not evident.

ACKNOWLEDGEMENTS

Financial support from the National Swedish Graduate School on Electronics Production (EPROPER) funded by the National Swedish Foundation for Strategic Research (SSF) is gratefully acknowledged.

REFERENCES

1. H. Kristiansen and J. Liu, *IEEE Trans. Comp. Packag. Manufact. Technol. A* 21, 208 (1998).
2. R.L. Keusseyan, J.L. Dilday, and B.S. Speck, *Int. J. Microcirc. Electron. Packag.* 17, 236 (1994).
3. O. Russanen and J. Lenkkeri, *IEEE Trans. Comp. Packag. Manufact. Technol. B* 18, 320 (1995).
4. D.J. Xie, *Microelectron. Reliab.* 40, 1191 (2000).
5. J.H. Constable, T. Kache, H. Teichmann, S. Muhle, and M.A. Gaynes, *IEEE Trans. Comp. Packag. Technol.* 22, 191 (1999).
6. T. Mori and K. Tanaka, *Acta Metall.* 21, 571 (1973).
7. D. Lu, Q.K. Tong, and C.P. Wong, *IEEE Trans. Electron. Packag. Manufact.* 22, 223 (1999).
8. Z. Wang, T.K. Chen, and D.J. Lloyd, *Metall. Trans. A* 24A, 197 (1993).
9. Y.T. Cho, K. Tohgo, and H. Ishii, *Acta Metall.* 45, 4787 (1997).
10. T.J. Zhang, Q.P. Zeng, X.N. Mao, and S.K. Cheng, *Rare Met. Mater. Eng.* 26, 18 (1997).
11. K.X. Hu, C.P. Yeh, and K.W. Wyatt, *IEEE Trans. Comp. Packag. Manufact. Technol. A* 20, 470 (1997).
12. E. Sancaktar and Y. Wei, *J. Adhesion Sci. Technol.* 10, 1221 (1996).
13. L.H. He and C.W. Lim, *Compos. Sci. Technol.* 61, 579 (2001).
14. E. Ghassemieh, *Compos. Sci. Technol.* 62, 67 (2002).